NAVAL POSTGRADUATE SCHOOL
Monterey, California

The Control of Parallel-Connected Inverters for U.S. Navy Shipboard Applications

by

John G. Ciezki
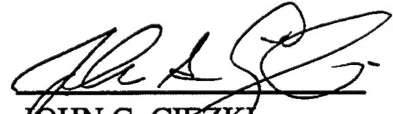Robert W. Ashton

April 18, 2001

20020227 209

NAVAL POSTGRADUATE SCHOOL
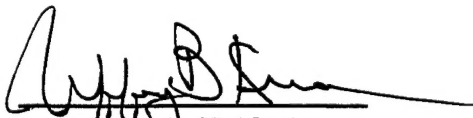## Monterey, California

RADM DAVID R. ELLISON
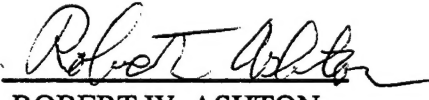Superintendent

R. Elster
Provost

This report was sponsored by the Naval Surface Warfare Center Carderock Division.

Approved for public release; distribution is unlimited.

The report was prepared by:

JOHN G. CIEZKI
Associate Professor
Department of Electrical and
Computer Engineering

ROBERT W. ASHTON
Associate Professor
Department of Electrical and
Computer Engineering

Reviewed by:

Released by:

JEFFREY B. KNORR
Chairman
Department of Electrical and
Computer Engineering

DAVID W. NETZER
Associate Provost and
Dean of Research

REPORT DOCUMENTATION PAGE

Form Approved
OMB No. 0704-0188

1. AGENCY USE ONLY (Leave blank)	2. REPORT DATE April 18, 2001	3. REPORT TYPE AND DATES COVERED Technical Report	

4. TITLE AND SUBTITLE
The Control of Parallel-Connected Inverters for U.S. Navy Shipboard Applications

5. FUNDING NUMBERS
N655400WR81000

6. AUTHOR(S)
John G. Ciezki and Robert W. Ashton

7. PERFORMING ORGANIZATION NAME(S) AND ADDRESS(ES)

Department of Electrical and Computer Engineering
Naval Postgraduate School
Monterey, CA 93943-5000

8. PERFORMING ORGANIZATION REPORT NUMBER

NPS-EC-01-003

9. SPONSORING/MONITORING AGENCY NAME(S) AND ADDRESS(ES)
Naval Surface Warfare Center Carderock Division
Code 812, Building 77L
Philadelphia Naval Business Center
Philadelphia, PA 19112-5083

10. SPONSORING/MONITORING AGENCY REPORT NUMBER

11. SUPPLEMENTARY NOTES
The views expressed in this report are those of the author and do not reflect the official policy or position of the Department of Defense or the United States Government.

12a. DISTRIBUTION/AVAILABILITY STATEMENT
Approved for public release; distribution is unlimited.

12b. DISTRIBUTION CODE

A

13. ABSTRACT (Maximum 200 words)

Concepts such as the Integrated Power System (IPS) and the DC Zonal Electric Distribution System (DC ZEDS) have motivated the study of power inverter control and paralleling strategies by the U.S. Navy. For example, in DC ZEDS a Ship Service Inverter Module (SSIM) converts DC power into AC power for use within a zone. For reasons of redundancy and logistics, multiple paralleled inverter submodules are used to implement the SSIM. The current effort supports ongoing SSIM hardware development by the SatCon Corporation. This report documents the modeling and control analysis of a set of parallel-connected PWM inverters. Although initially focusing on a static three-phase R-L load, the analysis is extended to three-phase symmetrical induction machine loads and three-phase round-rotor permanent-magnet synchronous machine loads. In each case, an algorithm for designing the local inner current control is developed by employing reference frame theory, replacing the paralleled inverters by an equivalent unit, and executing a nonlinear pole-placement strategy. Upon reviewing the equations necessary for AC machine vector control, the report concludes by documenting the analysis and design of a simple speed control loop for this aforementioned machine loads.

14. SUBJECT TERMS
PWM inverter, parallel, current control, vector control

15. NUMBER OF PAGES
44

16. PRICE CODE

17. SECURITY CLASSIFICATION OF REPORT Unclassified	18. SECURITY CLASSIFICATION OF THIS PAGE Unclassified	19. SECURITY CLASSIFICATION OF ABSTRACT Unclassified	20. LIMITATION OF ABSTRACT SAR

Table of Contents

I. INTRODUCTION

Significant advancements in power electronic devices, electric machine design, and power converter packaging have made it possible for the U.S. Navy to consider electric drive for its new land-attack destroyer, DD-21. Many of the benefits of electric drive stem from incorporating it into an Integrated Power System (IPS), where both ship service and ship propulsion power are derived from a common set of prime movers. The commercial marine industry, including Alstom, ABB and Siemens, has exploited the benefits of IPS for more than a decade in cruise liners, ferries, tankers, and research vessels. The advantages of IPS are manifold including: reduced lifecycle costs, flexible ship layout, cross-connect capability, reduced signature, optimized prime mover operation, simple and rapid propeller control, and a pool of available electric power for future electric auxiliaries and weapons.

In addition to the innovation of IPS, the U.S. Navy is also considering new paradigms in power distribution. In particular, traditional AC radial distribution architectures are being replaced by AC zonal architectures. The concept of a DC Zonal Electric Distribution System (DC ZEDS) is being investigated and advocated for its improved fault-response speed and distributed intelligence. Initiatives such as electric drive, IPS and DC ZEDS depend on the maturation of certain enabling technologies. A partial list includes power devices, compact high-bandwidth power converter topologies, high-power low-speed electric machinery, reliable automation technology, and advanced control and decision-making algorithms.

The research effort reported on in this document concentrates on developing models and analyses required to control multiple power inverters operating in parallel. One potential application for such work is the main Propulsion Motor Module (PMM). The PMM may consist of an AC motor driven by a DC-AC power inverter. One option for such an inverter is to employ a high-power slower-switching main inverter in parallel with a lower-power fast-switching inverter. The rationale for such a choice is explained as follows. A typical surface combatant may require on the order of 100,000 SHP to achieve full speed (50,000 SHP per shaft), indicating a PMM power rating of approximately 40MW. In order to achieve high-fidelity machine waveforms and rapid control, high-bandwidth (fast-switching) power converters are required. At high power, this implies IGBT technology. Unfortunately, to achieve 20kHz or greater device switching, IGBT-based inverters are limited to about 2MW. Despite the fact that the machine may be divided into more than three separate windings (phases), this would still require multiple paralleled modules and an unacceptably large-volume solution. For high power, devices must then be series connected, resulting in much lower admissible switching frequencies. One compromise then is to provide the "bulk" power of the drive using a slow-switching high-power inverter. The waveform fidelity could then be assured by paralleling with a fast-switching lower-power unit which may have to process no more than 10% of the rated

power. Thus the main "bulk" inverter would be rated at ~36MW and the "high-fidelity" inverter would be rated at ~4MW, theoretically realizable by two units in parallel. The "high-fidelity" unit would "fill in" the waveform distortion produced by the "bulk" unit which is constrained to switch at 1-2kHz.

Another application that may require paralleled inverters is DC ZEDS. In DC ZEDS, DC-to-AC inverters convert the interzonal DC voltage to the necessary AC voltage amplitudes and frequencies. To avoid developing and inventorying inverters of many different power ratings and to implement redundancy in the distribution system, inverters are paralleled. High-switching frequency units are required to achieve suitable AC waveforms to optimize efficiency and minimize the acoustic signature of auxiliary systems.

In order to tackle the problem paralleling, several questions must be posed: Will the units be co-located and, therefore, can they share information? If they are completely autonomous, how are they synchronized and how are the reference settings (i.e., voltage, current) determined? What strategy will be used to ensure proper load sharing? The following effort imposes the following boundaries on this problem: First, the units are assumed to be co-located as illustrated in Figure 1. Note that in Figure 1 the three-phase outputs of each unit are designated by a single connection line. Coupling inductors are used to aid in proper sharing and to limit unwanted circulating currents between the units. A common DC voltage input is then applied to each individual inverter unit. Second, an inner current control is assumed regardless of the type of load. With identical inverter units, this implies that each unit should produce an equal portion of the commanded load current. Third, a master control, also co-located, will produce the commanded current signals for each unit and establish the common electrical angle to ensure synchronization. As a consequence, if a fault occurs at one unit or it fails, the master control is responsible for re-allocating the current requirement between the remaining units within the bounds of their ratings. Furthermore, by assuming co-located units, the assertion of a co-located master controller is not unreasonable. Also, this does not prohibit a fall-back local droop control should the master fail. The assumed "global" or master control is indicated in Figure 2, where separate q- and d-commanded currents are specified in the synchronous reference frame (outlined later in this document). The quantity ω_e^* is the commanded electrical radian frequency which could be a constant or could be a variable, say in a variable-speed drive. The fourth and final assumption is that the local control will appropriately handle circulating or zero-sequence currents. The local control refers to how the commanded currents at each "local" unit are converted into actual switch gate signals. One approach to such a local control is illustrated in Figure 3. The actual inverter output currents (i_{a1}, i_{b1}, i_{c1}) are fed back to the local control. After being transformed into the synchronous reference frame, they are compared with the desired current values ("desired" is designated by an asterisk).
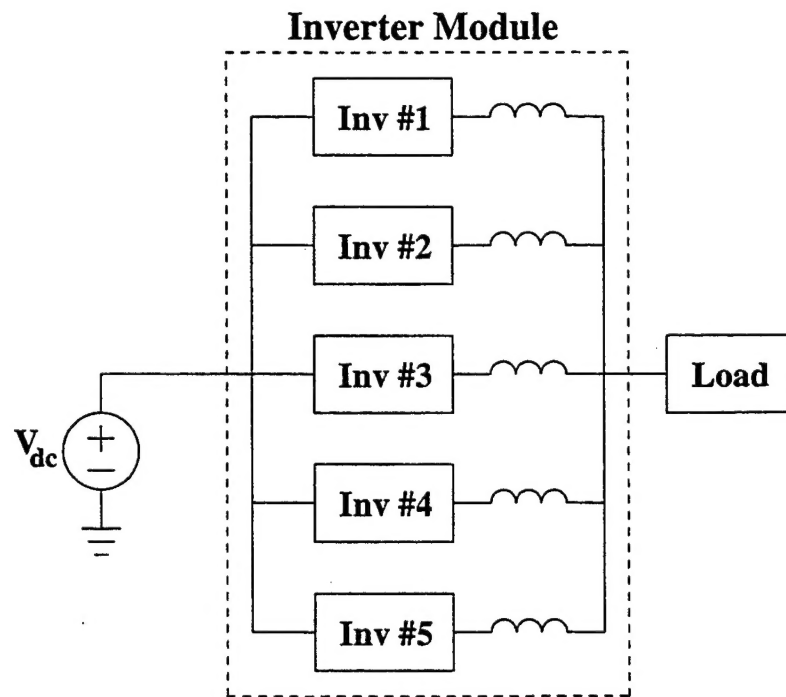
Inverter Module

Figure 1. Inverter module containing five inverter submodules
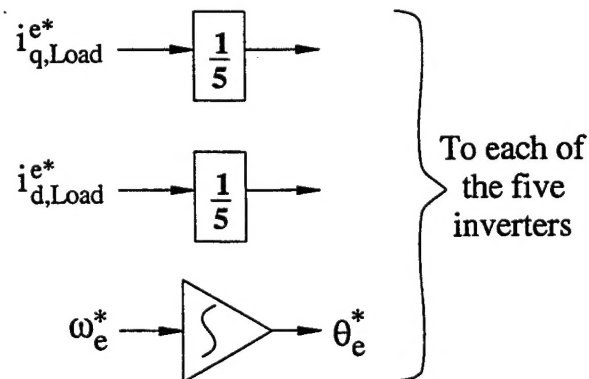
Figure 2. Synchronizing and sharing global control
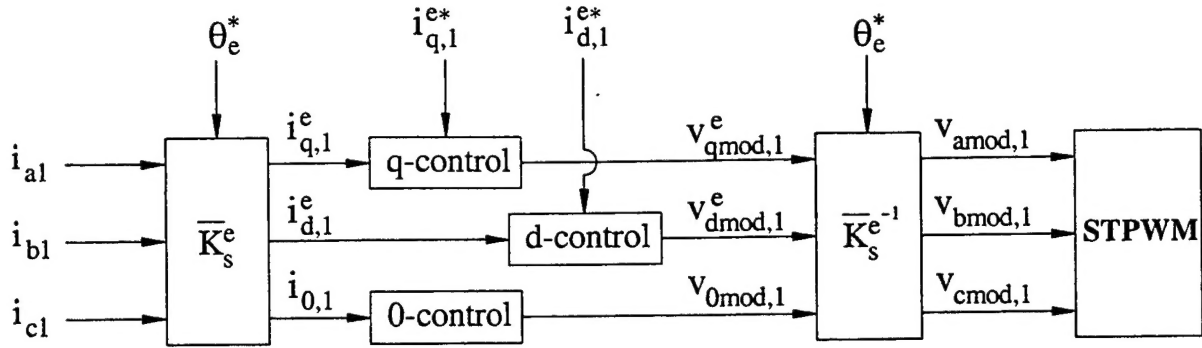
Figure 3. QD0 local control

The qd0-controllers produce modulating signals which are then inverse transformed back into "physical" (abc) variables which, for instance, can then be used in a standard Sine-Triangle Pulse-Width-Modulation (STPWM) algorithm. Other approaches including Space Vector Modulation are easily substituted into the block diagram.

The principal goal of this work is to establish a theoretical basis for the stability of a particular control implementation, while in the process evolving the necessary system modeling equations required for detailed simulation. The initial development is conducted for a generic three-phase Resistor-Inductor (R-L) load, but since many different three-phase loads are admissible for shipboard applications, the results are then extended to a generic three-phase induction machine and a generic three-phase permanent-magnet synchronous machine. The following details are presented in this document:

- the dynamic equations are developed for two inverters powering an R-L load (given an assumed local current control);

- an equivalent single-inverter system is derived and gains are analytically determined;

- a mechanism for mapping the single-inverter gains to a multiple number of paralleled inverters is outlined and verified;

- the local zero-sequence control is designed to handle components of the potential circulating currents;

- the above results are extended to a symmetrical three-phase induction machine load;

- the above results are extended to a round-rotor three-phase permanent-magnet synchronous machine load;

- the necessary equations for the vector-control of induction machines and permanent-magnet synchronous machines are outlined;

- the design of an outer speed-control loop appropriate to each machine type is presented.

Much of the aforementioned development is equation and reference frame intensive. Many intermediate steps are included to provide guidance for any future modifications or extensions of this work (i.e., different loads or different control strategies).

II. TWO PARALLELED INVERTERS POWERING AN R-L LOAD

The basic system under consideration is illustrated in Figure 4. Note, the inverters share a common DC source bus and each is coupled to the R-L load through inductors labeled L_1 and L_2. The voltage $v_{ao,1}$ is referenced from the center of the a-phase leg (of unit 1) to a fictitious mid-point of the DC voltage supply (designated o). These voltages are sometimes referred to as "pole voltages." The load is assumed to be wye-connected with the neutral point (labelled n) left floating.
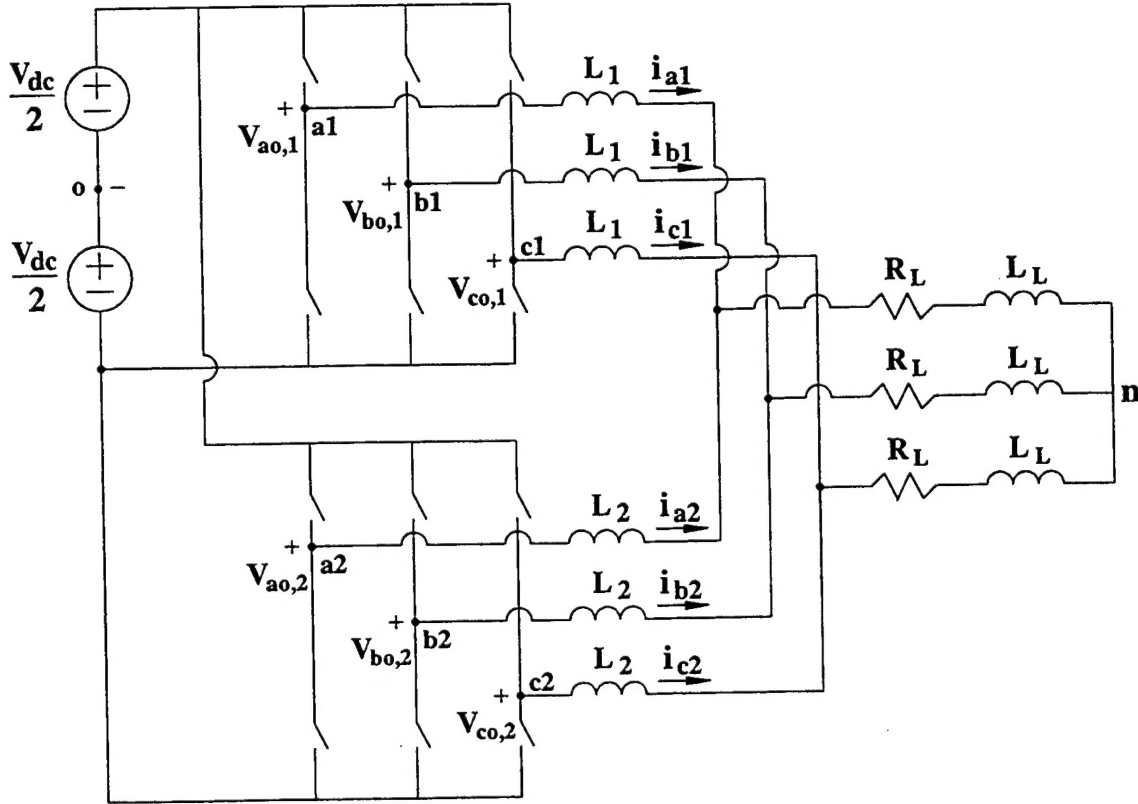

Figure 4. Two paralleled inverters powering an R-L load

Since the interconnection of inductances L_1, L_2 and L_L form a cutset, all three inductor currents cannot be state variables. Thus, one is eliminated by virtue of the algebraic constraint. If we choose the currents in L_1 and L_2 as our state variables, the dynamics of the circuit portrayed in Figure 4 can be established.

A. Circuit Representation in Physical Variables

The following Kirchhoff's Voltage Law (KVL) loop equations may be written for the network:

$$-v_{ao,1} + L_1 \frac{d}{dt} i_{a1} + R_L (i_{a1} + i_{a2}) + L_L \frac{d}{dt} (i_{a1} + i_{a2}) + v_{no} = 0 \tag{1}$$

$$-v_{bo,1} + L_1 \frac{d}{dt} i_{b1} + R_L (i_{b1} + i_{b2}) + L_L \frac{d}{dt} (i_{b1} + i_{b2}) + v_{no} = 0 \tag{2}$$

$$-v_{co,1} + L_1 \frac{d}{dt} i_{c1} + R_L (i_{c1} + i_{c2}) + L_L \frac{d}{dt} (i_{c1} + i_{c2}) + v_{no} = 0 \tag{3}$$

$$-v_{ao,1} + L_1 \frac{d}{dt} i_{a1} - L_2 \frac{d}{dt} i_{a2} + v_{ao,2} = 0 \tag{4}$$

$$-v_{bo,1} + L_1 \frac{d}{dt} i_{b1} - L_2 \frac{d}{dt} i_{b2} + v_{bo,2} = 0 \tag{5}$$

$$-v_{co,1} + L_1 \frac{d}{dt} i_{c1} - L_2 \frac{d}{dt} i_{c2} + v_{co,2} = 0 \tag{6}$$

Equations (1)-(6) may be expressed in vector notation as:

$$-\vec{v}_{abco,1} + L_1 \frac{d}{dt} \vec{i}_{abc,1} + R_L (\vec{i}_{abc,1} + \vec{i}_{abc,2}) + L_L (\frac{d}{dt} \vec{i}_{abc,1} + \frac{d}{dt} \vec{i}_{abc,2}) + \begin{bmatrix} v_{no} \\ v_{no} \\ v_{no} \end{bmatrix} = \vec{0} \tag{7}$$

$$-\vec{v}_{abco,1} + L_1 \frac{d}{dt} \vec{i}_{abc,1} - L_2 \frac{d}{dt} \vec{i}_{abc,2} + \vec{v}_{abco,2} = \vec{0} \tag{8}$$

where for instance $\vec{i}_{abc,1} = [i_{a1}, i_{b1}, i_{c1}]^T$ and $\vec{v}_{abco,1} = [v_{ao,1}, v_{bo,1}, v_{co,1}]^T$. The voltage v_{no} is the voltage from the neutral point of the load back around to the mid-point of the DC voltage supply.

B. Circuit Representation in the Synchronous Reference Frame

These equations may be transformed into the synchronous reference frame (designated by the superscript "e") using the identities

$$\vec{v}_{qd0,1}^e = \overline{K}_s^e \vec{v}_{abco,1} \tag{9}$$

$$\vec{v}_{qd0,2}^e = \overline{K}_s^e \vec{v}_{abco,2} \tag{10}$$

$$\vec{i}_{qd0,1}^e = \overline{K}_s^e \vec{i}_{abc,1} \tag{11}$$

$$\vec{i}_{qd0,2}^e = \overline{K}_s^e \vec{i}_{abc,2} \tag{12}$$

where the diffeomorphic transformation matrix $\overline{K}_s^e$ is given by

$$\overline{K}_s^e = \begin{bmatrix} \dfrac{2}{3}\cos\theta_e & \dfrac{2}{3}\cos(\theta_e - \dfrac{2\pi}{3}) & \dfrac{2}{3}\cos(\theta_e + \dfrac{2\pi}{3}) \\[2mm] \dfrac{2}{3}\sin\theta_e & \dfrac{2}{3}\sin(\theta_e - \dfrac{2\pi}{3}) & \dfrac{2}{3}\sin(\theta_e + \dfrac{2\pi}{3}) \\[2mm] \dfrac{1}{3} & \dfrac{1}{3} & \dfrac{1}{3} \end{bmatrix} \tag{13}$$

and, for instance, the notation implies that $\vec{v}_{qd0,1}^e = [v_{q,1}^e, v_{d,1}^e, v_{0,1}]^T$. The zero-sequence quantity (i.e., $v_{0,1}$) is generally not given a superscript since it is equivalent in every reference frame. The angle θ_e varies at a radian frequency of ω_e, which for instance, would be the fundamental or desired output frequency of the inverters. Solving for the "abc" quantities in (9)-(12) and then substituting into (7)-(8) gives:

$$-(\overline{K}_s^e)^{-1}\vec{v}_{qd0,1}^e + (L_1 + L_L)\frac{d}{dt}\left[(\overline{K}_s^e)^{-1}\vec{i}_{qd0,1}^e\right] + R_L(\overline{K}_s^e)^{-1}\vec{i}_{qd0,1}^e + \tag{14}$$

$$R_L(\overline{K}_s^e)^{-1}\vec{i}_{qd0,2}^e + L_L\frac{d}{dt}\left[(\overline{K}_s^e)^{-1}\vec{i}_{qd0,2}^e\right] + \begin{bmatrix} v_{no} \\ v_{no} \\ v_{no} \end{bmatrix} = \vec{0}$$

$$-(\overline{K}_s^e)^{-1}\vec{v}_{qd0,1}^e + L_1\frac{d}{dt}\left[(\overline{K}_s^e)^{-1}\vec{i}_{qd0,1}^e\right] - \tag{15}$$

$$L_2\frac{d}{dt}\left[(\overline{K}_s^e)^{-1}\vec{i}_{qd0,2}^e\right] + (\overline{K}_s^e)^{-1}\vec{v}_{qd0,2}^e = \vec{0}$$

Multiplying (14)-(15) by $\overline{K}_s^e$ and employing the product rule illustrated in (16)

$$\frac{d}{dt}\left[(\overline{K}_s^e)^{-1}\vec{i}_{qd0,1}^e\right] = (\overline{K}_s^e)^{-1}\frac{d}{dt}\vec{i}_{qd0,1}^e + \frac{d}{dt}(\overline{K}_s^e)^{-1}\vec{i}_{qd0,1}^e \tag{16}$$

gives

$$-\vec{v}_{qd0,1}^e + (L_1 + L_L)\frac{d}{dt}\vec{i}_{qd0,1}^e + (L_1 + L_L)\overline{K}_s^e\frac{d}{dt}\left[(\overline{K}_s^e)^{-1}\right]\vec{i}_{qd0,1}^e + \tag{17}$$

$$R_L(\vec{i}_{qd0,1}^e + \vec{i}_{qd0,2}^e) + L_L\overline{K}_s^e\frac{d}{dt}\left[(\overline{K}_s^e)^{-1}\right]\vec{i}_{qd0,2}^e + \overline{K}_s^e\begin{bmatrix} v_{no} \\ v_{no} \\ v_{no} \end{bmatrix} = \vec{0}$$

$$-\vec{v}_{qd0,1}^e + L_1\frac{d}{dt}\vec{i}_{qd0,1}^e + L_1\overline{K}_s^e\frac{d}{dt}\left[(\overline{K}_s^e)^{-1}\right]\vec{i}_{qd0,1}^e - \tag{18}$$

$$L_2\frac{d}{dt}\vec{i}_{qd0,2}^e - L_2\overline{K}_s^e\frac{d}{dt}\left[(\overline{K}_s^e)^{-1}\right]\vec{i}_{qd0,2}^e + \vec{v}_{qd0,2}^e = \vec{0}$$

Equations (17) and (18) are simplified by observing that

$$\overline{K}_s^e\frac{d}{dt}(\overline{K}_s^e)^{-1} = \begin{bmatrix} 0 & \omega_e & 0 \\ -\omega_e & 0 & 0 \\ 0 & 0 & 0 \end{bmatrix} \tag{19}$$

and

$$\overline{K}_s^e \begin{bmatrix} v_{no} \\ v_{no} \\ v_{no} \end{bmatrix} = \begin{bmatrix} 0 \\ 0 \\ v_{no} \end{bmatrix} \tag{20}$$

Thus, expanding the resultant vector equations gives the representation of the two-inverter system in the synchronous reference frame:

$$-v_{q,1}^e + (L_1 + L_L)\frac{d}{dt}i_{q,1}^e + (L_1 + L_L)\omega_e i_{d,1}^e + \tag{21}$$

$$R_L(i_{q,1}^e + i_{q,2}^e) + L_L\frac{d}{dt}i_{q,2}^e + L_L\omega_e i_{d,2}^e = 0$$

$$-v_{d,1}^e + (L_1 + L_L)\frac{d}{dt}i_{d,1}^e - (L_1 + L_L)\omega_e i_{q,1}^e + \tag{22}$$

$$R_L(i_{d,1}^e + i_{d,2}^e) + L_L\frac{d}{dt}i_{d,2}^e - L_L\omega_e i_{q,2}^e = 0$$

$$-v_{0,1} + (L_1 + L_L)\frac{d}{dt}i_{0,1} \ R_L(i_{0,1} + i_{0,2}) + L_L\frac{d}{dt}i_{0,2} + v_{no} = 0 \tag{23}$$

$$-v_{q,1}^e + L_1\frac{d}{dt}i_{q,1}^e + L_1\omega_e i_{d,1}^e - L_2\frac{d}{dt}i_{q,2}^e - L_2\omega_e i_{d,2}^e + v_{q,2}^e = 0 \tag{24}$$

$$-v_{d,1}^e + L_1\frac{d}{dt}i_{d,1}^e - L_1\omega_e i_{q,1}^e - L_2\frac{d}{dt}i_{d,2}^e + L_2\omega_e i_{q,2}^e + v_{d,2}^e = 0 \tag{25}$$

$$-v_{0,1} + L_1\frac{d}{dt}i_{0,1} - L_2\frac{d}{dt}i_{0,2} + v_{0,2} = 0 \tag{26}$$

Recall, the voltages $v_{q,1}^e$ and $v_{d,1}^e$ are the transformed inverter #1 pole voltages while $v_{0,1}$ is the zero-sequence voltage for that unit.

With a wye-connected load, Kirchhoff's Current Law (KCL) demands that

$$(i_{a1} + i_{a2}) + (i_{b1} + i_{b2}) + (i_{c1} + i_{c2}) = 0 \tag{27}$$

But from the identities (11)-(12), the inverter zero-sequence currents relate to the output currents by

$$i_{0,1} = \frac{1}{3}\left[i_{a1} + i_{b1} + i_{c1}\right] \tag{28}$$

$$i_{0,2} = \frac{1}{3}\left[i_{a2} + i_{b2} + i_{c2}\right] \tag{29}$$

so that (27) then implies that

$$i_{0,2} = -i_{0,1} \tag{30}$$

Therefore, the inverter #2 zero-sequence current is NOT an independent state variable, but instead is algebraically related to $i_{0,1}$. This is a direct consequence of the wye-connection of the load with the neutral floating. Substituting (30) into (26) gives

$$-v_{0,1} + L_1 \frac{d}{dt} i_{0,1} + L_2 \frac{d}{dt} i_{0,1} + v_{0,2} = 0 \tag{31}$$

which simplifies down to

$$\frac{d}{dt} i_{0,1} = \frac{v_{0,1} - v_{0,2}}{L_1 + L_2} \tag{32}$$

Thus, any difference between the developed zero-sequence voltages of the units will result in a zero-sequence current, which must flow between the units. Furthermore substituting (30) into (23) results in

$$-v_{0,1} + L_1 \frac{d}{dt} i_{0,1} + v_{no} = 0 \tag{33}$$

which allows us to solve for v_{no} by first substituting (32)

$$v_{no} = v_{0,1} - \frac{L_1}{L_1 + L_2} \left[v_{0,1} - v_{0,2} \right] \tag{34}$$

or more compactly

$$v_{no} = \frac{L_2 v_{0,1} + L_1 v_{0,2}}{L_1 + L_2} \tag{35}$$

The dynamic governing the zero-sequence current is described by (32) while the remaining state variable equations, (21)-(22) and (24)-(25), may be rewritten in vector/matrix form as

$$\bar{L}_a \frac{d}{dt} \vec{i}^e_{q,12} = \bar{R}_a \vec{i}^e_{q,12} - \omega_e \bar{L}_a \vec{i}^e_{d,12} + \bar{C}_a \vec{v}^e_{q,12} \tag{36}$$

$$\bar{L}_a \frac{d}{dt} \vec{i}^e_{d,12} = \omega_e \bar{L}_a \vec{i}^e_{q,12} + \bar{R}_a \vec{i}^e_{d,12} + \bar{C}_a \vec{v}^e_{d,12} \tag{37}$$

where

$$\vec{i}^e_{q,12} = \begin{bmatrix} i^e_{q,1} \\ i^e_{q,2} \end{bmatrix} \tag{38}$$

$$\vec{i}^e_{d,12} = \begin{bmatrix} i^e_{d,1} \\ i^e_{d,2} \end{bmatrix} \tag{39}$$

$$\vec{v}^e_{q,12} = \begin{bmatrix} v^e_{q,1} \\ v^e_{q,2} \end{bmatrix} \tag{40}$$

$$\vec{v}^e_{d,12} = \begin{bmatrix} v^e_{d,1} \\ v^e_{d,2} \end{bmatrix} \tag{41}$$

and

$$\bar{L}_a = \begin{bmatrix} L_1 + L_L & L_L \\ L_1 & -L_2 \end{bmatrix} \tag{42}$$

$$\overline{R}_a = \begin{bmatrix} -R_L & -R_L \\ 0 & 0 \end{bmatrix} \tag{43}$$

$$\overline{C}_a = \begin{bmatrix} 1 & 0 \\ 1 & -1 \end{bmatrix} \tag{44}$$

Equations (36)-(37) may be placed into state-space normal form

$$\frac{d}{dt} \vec{i}^e_{q,12} = \overline{L}_a^{-1} \overline{R}_a \vec{i}^e_{q,12} - \omega_e \vec{i}^e_{d,12} + \overline{L}_a^{-1} \overline{C}_a \vec{v}^e_{q,12} \tag{45}$$

$$\frac{d}{dt} \vec{i}^e_{d,12} = \omega_e \vec{i}^e_{q,12} + \overline{L}_a^{-1} \overline{R}_a \vec{i}^e_{d,12} + \overline{L}_a^{-1} \overline{C}_a \vec{v}^e_{d,12} \tag{46}$$

where for the reader's information

$$\overline{L}_a^{-1} \overline{R}_a = \begin{bmatrix} \dfrac{R_L L_2}{L_{den}} & \dfrac{R_L L_2}{L_{den}} \\ \dfrac{R_L L_1}{L_{den}} & \dfrac{R_L L_1}{L_{den}} \end{bmatrix} \tag{47}$$

$$\overline{L}_a^{-1} \overline{C}_a = \begin{bmatrix} \dfrac{-L_2 - L_L}{L_{den}} & \dfrac{L_L}{L_{den}} \\ \dfrac{L_L}{L_{den}} & \dfrac{-L_1 - L_L}{L_{den}} \end{bmatrix} \tag{48}$$

and

$$L_{den} = -L_1 L_2 - L_L L_2 - L_1 L_L \tag{49}$$

Thus, from (45)-(46) we observe that the "q" and "d" dynamics are coupled by the "speed current" terms $\omega_e \vec{i}^e_{q,12}$ and $\omega_e \vec{i}^e_{d,12}$.

C. Synchronous Reference Frame Control Equations

In order to investigate the stability of a proposed control architecture and to select suitable control gains, the control dynamics must be modeled and linked to equations (45)-(46). Assume that each inverter unit is supplied a common synchronous reference frame angle θ_e, which can then be used locally together with the inverter output currents to calculate the inverter's qd-currents (see Figures 2 and 3). These currents may then be compared against desired qd-synchronous reference frame currents and processed through a Proportional-plus-Integral (PI) controller. The outputs, still mathematically in the synchronous reference frame, would then be inverse transformed back into abc-frame (physical) variables, which could serve as the modulating signals in a Sine-Triangle Pulse-Width-Modulation (STPWM) strategy (see Figure 3). A PI-control is used since for sinusoidal reference abc-currents, the commanded qd-currents are constants in the synchronous reference frame. Thus, the integral action will guarantee zero steady-state error, while the proportional action guarantees improved stability margin. The

implementation of the integrator must account for "integrator windup" which may occur when large operating point changes are specified.

Given a bipolar triangle waveform varying between A_t and $-A_t$, the control is said to remain in the "linear modulation" range as long as each modulation signal has magnitude less than A_t. If the control is constrained to operate in the "linear modulation" range, then the following relates the fundamental modulation signal to the respective fundamental inverter output line-to-neutral voltage (as long as the fundamental frequency is much lower than the carrier frequency):

$$\begin{bmatrix} v_{a1,n} \\ v_{b1,n} \\ v_{c1,n} \end{bmatrix} = \frac{V_{dc}}{2\,A_t} \begin{bmatrix} v_{amod,1} \\ v_{bmod,1} \\ v_{cmod,1} \end{bmatrix} \tag{50}$$

The frequency spectra for the line-to-neutral voltages is identical to the pole voltages except for the triplen harmonics. Therefore, the fundamentals are identical and would thus be also related by (50). Transforming (50) into the synchronous reference frame gives us the "average" qd-voltage relationships:

$$\begin{bmatrix} v_{q,1}^e \\ v_{d,1}^e \\ v_{0,1} \end{bmatrix} = \frac{V_{dc}}{2\,A_t} \begin{bmatrix} v_{qmod,1}^e \\ v_{dmod,1}^e \\ v_{0mod,1} \end{bmatrix} \tag{51}$$

The term $K_{pwm} = \dfrac{V_{dc}}{2\,A_t}$ is termed the STPWM gain and is clearly a function of the inverter input DC voltage and the amplitude of the carrier triangle waveform (clearly this modulation may take place via a Digital Signal Processing implementation and therefore the amplitude A_t is dictated by the programmer). The dynamics of the PI-control and the interface with the modeling equations (45)-(46) are therefore given by:

$$\frac{d}{dt} x_{q,1}^e = i_{q,1}^{e*} - i_{q,1}^e \tag{52}$$

$$\frac{d}{dt} x_{d,1}^e = i_{d,1}^{e*} - i_{d,1}^e \tag{53}$$

$$\frac{d}{dt} x_{q,2}^e = i_{q,2}^{e*} - i_{q,2}^e \tag{54}$$

$$\frac{d}{dt} x_{d,2}^e = i_{d,2}^{e*} - i_{d,2}^e \tag{55}$$

$$v_{q,1}^e = K_{pwm} K_{pq} \left[i_{q,1}^{e*} - i_{q,1}^e \right] + K_{pwm} K_{iq} x_{q,1}^e \tag{56}$$

$$v_{d,1}^e = K_{pwm} K_{pd} \left[i_{d,1}^{e*} - i_{d,1}^e \right] + K_{pwm} K_{id} x_{d,1}^e \tag{57}$$

$$v_{q,2}^e = K_{pwm} K_{pq} \left[i_{q,2}^{e*} - i_{q,2}^e \right] + K_{pwm} K_{iq} x_{q,2}^e \tag{58}$$

$$v_{d,2}^e = K_{pwm} K_{pd} \left[i_{d,2}^{e*} - i_{d,2}^e \right] + K_{pwm} K_{id} x_{d,2}^e \tag{59}$$

where the quantities with "*" denote commanded or desired values. The resultant set of equations, (45)-(46) and (52)-(59) provide the 8th-order system of equations in state-space normal form. As long as the average qd-voltages adequately represent the bulk of the dynamics, the eigenvalues of the resultant system matrix characterize the stability of the interconnected inverters and load. Reiterating, these equations would not be used for detailed simulation since we have average-value modeled through the inverter; however, the other purpose of modeling is to facilitate control design, which is what we are setting the stage to do here. Those equations take the form:

$$\frac{d}{dt} \vec{i}_{q,12}^e = \overline{A}_1 \vec{i}_{q,12}^e - \omega_e \vec{i}_{d,12}^e + K_{iq}' \overline{A}_2 \vec{x}_{q,12}^e + K_{pq}' \overline{A}_2 \vec{i}_{q,12}^{e*} \tag{60}$$

$$\frac{d}{dt} \vec{i}_{d,12}^e = \omega_e \vec{i}_{q,12}^e + \overline{A}_3 \vec{i}_{d,12}^e + K_{id}' \overline{A}_2 \vec{x}_{d,12}^e + K_{pd}' \overline{A}_2 \vec{i}_{d,12}^{e*} \tag{61}$$

$$\frac{d}{dt} \vec{x}_{q,12}^e = -\vec{i}_{q,12}^e + \vec{i}_{q,12}^{e*} \tag{62}$$

$$\frac{d}{dt} \vec{x}_{d,12}^e = -\vec{i}_{d,12}^e + \vec{i}_{d,12}^{e*} \tag{63}$$

where the "primed" gains are

$$K_{pq}' = K_{pwm} K_{pq} \tag{64}$$

$$K_{iq}' = K_{pwm} K_{iq} \tag{65}$$

$$K_{pd}' = K_{pwm} K_{pd} \tag{66}$$

$$K_{id}' = K_{pwm} K_{id} \tag{67}$$

Technically, as will be discussed further in this document, the primed gains may also be used to represent additional scaling effects such as the non-unity gain of current sensors. The matrices in (60)-(61) are given by

$$\overline{A}_1 = \begin{bmatrix} \dfrac{R_L L_2 + K_{pq}'(L_2 + L_L)}{L_{den}} & \dfrac{R_L L_2 - K_{pq}' L_L}{L_{den}} \\ \dfrac{R_L L_1 - K_{pq}' L_L}{L_{den}} & \dfrac{R_L L_1 + K_{pq}'(L_1 + L_L)}{L_{den}} \end{bmatrix} \tag{68}$$

$$\overline{A}_2 = \begin{bmatrix} \dfrac{L_2 + L_L}{L_{den}} & \dfrac{L_L}{L_{den}} \\ \dfrac{L_L}{L_{den}} & \dfrac{L_1 + L_L}{L_{den}} \end{bmatrix} \tag{69}$$

$$\overline{A}_3 = \begin{bmatrix} \dfrac{R_L L_2 + K_{pd}'(L_2 + L_L)}{L_{den}} & \dfrac{R_L L_2 - K_{pd}' L_L}{L_{den}} \\ \dfrac{R_L L_1 - K_{pd}' L_L}{L_{den}} & \dfrac{R_L L_1 + K_{pd}'(L_1 + L_L)}{L_{den}} \end{bmatrix} \tag{70}$$

The notation in (60)-(63) uses the vectors

$$\vec{x}_{q,12}^{e} = \begin{bmatrix} x_{q,1}^{e} \\ x_{q,2}^{e} \end{bmatrix} \tag{71}$$

$$\vec{x}_{d,12}^{e} = \begin{bmatrix} x_{d,1}^{e} \\ x_{d,2}^{e} \end{bmatrix} \tag{72}$$

$$\vec{i}_{q,12}^{e*} = \begin{bmatrix} i_{q,1}^{e*} \\ i_{q,2}^{e*} \end{bmatrix} \tag{73}$$

$$\vec{i}_{d,12}^{e*} = \begin{bmatrix} i_{d,1}^{e*} \\ i_{d,2}^{e*} \end{bmatrix} \tag{74}$$

The resultant system matrix takes the form:

$$\overline{A}_{sys} = \begin{bmatrix} \overline{A}_1 & -\omega_e \overline{I}_{2x2} & K_{iq}' \overline{A}_2 & \overline{0}_{2x2} \\ \omega_e \overline{I}_{2x2} & \overline{A}_3 & \overline{0}_{2x2} & K_{id}' \overline{A}_2 \\ -\overline{I}_{2x2} & \overline{0}_{2x2} & \overline{0}_{2x2} & \overline{0}_{2x2} \\ \overline{0}_{2x2} & -\overline{I}_{2x2} & \overline{0}_{2x2} & \overline{0}_{2x2} \end{bmatrix} \tag{75}$$

where $\overline{0}_{2x2}$ is a two-by-two null matrix and $\overline{I}_{2x2}$ is a two-by-two identity matrix. The eigenvalues of (75) dictate the stability and strongly influence the transient response characteristics of the system. We will illustrate in subsequent sections how manipulating the PI-control gains changes the eigenvalue locations.

III. DETERMINING THE CONTROL GAINS

In order to establish a set of gains for each unit, let's consider converting the two separate inverter units into a single quivalent. To do this, the per-phase steady-state equivalent circuit of Figure 5 is helpful. The Thevenin Equivalent circuit looking back from the load is depicted in Figure 6. If we assume near-identical units ($L_1 = L_2$ and equal voltages), then the Thevenin circuit reduces to simply the inverter voltage in series with half of the coupling inductance.
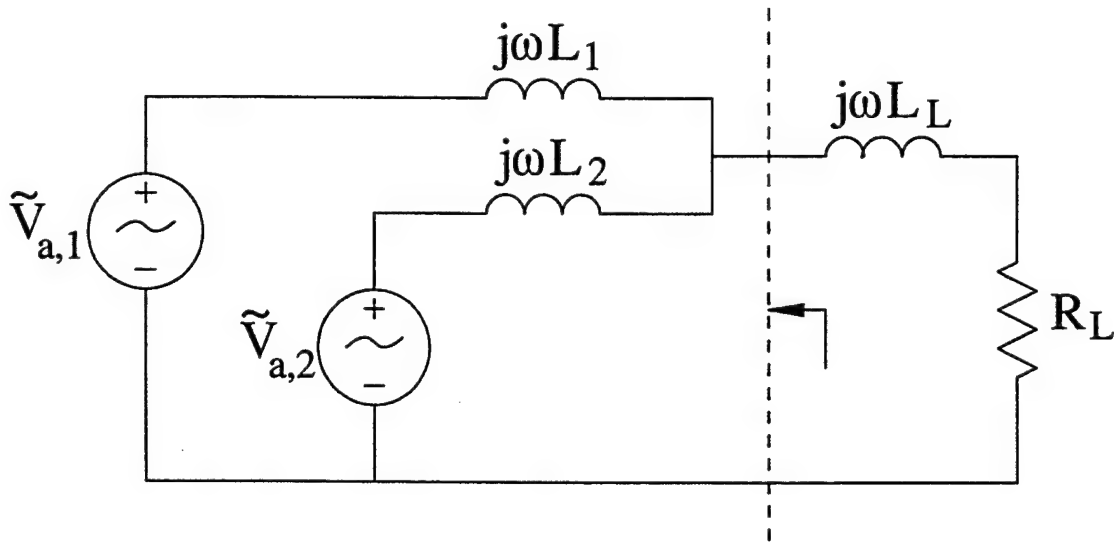
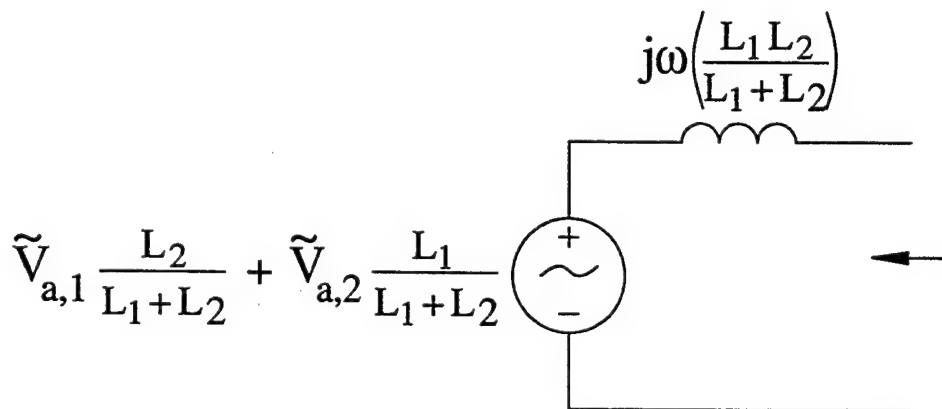**Figure 5. Per-phase steady-state equivalent circuit**

Figure 6. Per-phase steady-state Thevenin circuit

Thus, to represent two units by one equivalent, the connection inductance used for the equivalent must be one-half the inductance used for either channel. The following procedure is adopted:

- model the equations for a single inverter with connection inductance given by $L_x = \frac{1}{2}L_1$ (thus, for 2 units in parallel);

- given desired closed-loop pole locations, substitute the control model into this representation and solve for the two q-channel and the two d-channel gains;

- modify the gains to account for the fact that two inverters are used. This happens because each unit is only responsible for supplying half of the desired q- and d-axis load current.

To better illustrate the last bullet, a single aggregate inverter would have a q-axis modulating voltage established by:

$$v_{q,mod}^e = K_{iq} \int_0^t (i_q^{e*} - i_q^e)\,dt + K_{pq}(i_q^{e*} - i_q^e) \tag{76}$$

In a system with two paralleled inverters, the commanded current is dividely evenly between the units so that the q-axis modulating signal for unit one would be

$$v_{q,mod1}^e = K_{iq1} \int_0^t \left(\frac{i_q^{e*}}{2} - \frac{i_q^e}{2}\right)dt + K_{pq1}\left(\frac{i_q^{e*}}{2} - \frac{i_q^e}{2}\right) \tag{77}$$

or to make the point more explicit

$$v_{q,mod1}^e = \frac{K_{iq1}}{2} \int_0^t (i_q^{e*} - i_q^e)\,dt + \frac{K_{pq1}}{2}(i_q^{e*} - i_q^e) \tag{78}$$

Thus, for one of the two parallel units (designated with subscript 1) to produce the same voltage as the equivalent unit (no subscript number), it must follow then that

$$K_{iq} = \frac{K_{iq1}}{2} \tag{79}$$

$$K_{pq} = \frac{K_{pq1}}{2} \tag{80}$$

Therefore, upon finding the gains for a single unit, the gains for each of the two separate units are found by doubling those values. This point will be revisited during a subsequent example.

A. Equivalent Inverter System Equations

The development of the equations required to find the single-unit gains is presented next. The inductance L_x represents the single unit (or equivalent connection) inductance.

Omitting consideration of the zero-sequence dynamics (since with a wye-connected load and a single inverter, there would not be any), the voltage equations in the synchronous reference frame are given by:

$$-v_q^e + (L_x + L_L)\frac{d}{dt}i_q^e + (L_x + L_L)\omega_e i_d^e + R_L i_q^e = 0 \tag{81}$$

$$-v_d^e + (L_x + L_L)\frac{d}{dt}i_d^e - (L_x + L_L)\omega_e i_q^e + R_L i_d^e = 0 \tag{82}$$

or in state-space form

$$\frac{d}{dt}i_q^e = -\omega_e i_d^e - \frac{R_L}{L_x + L_L}i_q^e + \frac{1}{L_x + L_L}v_q^e \tag{83}$$

$$\frac{d}{dt}i_d^e = \omega_e i_q^e - \frac{R_L}{L_x + L_L}i_d^e + \frac{1}{L_x + L_L}v_d^e \tag{84}$$

Coupling these with the PI-control equations

$$\frac{d}{dt}x_q^e = i_q^{e*} - i_q^e \tag{85}$$

$$\frac{d}{dt}x_d^e = i_d^{e*} - i_d^e \tag{86}$$

$$v_q^e = K_{pwm}[K_{pq}(i_q^{e*} - i_q^e) + K_{iq}x_q^e] \tag{87}$$

$$v_d^e = K_{pwm}[K_{pd}(i_d^{e*} - i_d^e) + K_{id}x_d^e] \tag{88}$$

yields, in state-space normal form,

$$\frac{d}{dt}\begin{bmatrix} i_q^e \\ i_d^e \\ x_q^e \\ x_d^e \end{bmatrix} = \begin{bmatrix} \dfrac{-(R_L + K_{pq}')}{L_x + L_L} & -\omega_e & \dfrac{K_{iq}'}{L_x + L_L} & 0 \\[2mm] \omega_e & \dfrac{-(R_L + K_{pd}')}{L_x + L_L} & 0 & \dfrac{K_{id}'}{L_x + L_L} \\[2mm] -1 & 0 & 0 & 0 \\[1mm] 0 & -1 & 0 & 0 \end{bmatrix}\begin{bmatrix} i_q^e \\ i_d^e \\ x_q^e \\ x_d^e \end{bmatrix} \tag{89}$$

$$+ \begin{bmatrix} \dfrac{K_{pq}'}{L_x + L_L} & 0 \\[2mm] 0 & \dfrac{K_{pd}'}{L_x + L_L} \\[2mm] 1 & 0 \\[1mm] 0 & 1 \end{bmatrix}\begin{bmatrix} i_q^{e*} \\ i_d^{e*} \end{bmatrix}$$

where $K_{pq}' = K_{pwm}K_{pq}$ and $K_{iq}' = K_{pwm}K_{iq}$ have been used for notational simplicity.

B. A qd-Current Loop Design Strategy

Equation (89) can be further simplified if we assign

$$K_{pq}'' = \frac{R_L + K_{pq}'}{L_x + L_L} \tag{90}$$

$$K_{pd}^{''} = \frac{R_L + K_{pd}^{'}}{L_x + L_L} \tag{91}$$

$$K_{iq}^{''} = \frac{K_{iq}^{'}}{L_x + L_L} \tag{92}$$

$$K_{id}^{''} = \frac{K_{id}^{'}}{L_x + L_L} \tag{93}$$

The characteristic equation for (89) is then found to be

$$\lambda^4 + (K_{pq}^{''} + K_{pd}^{''})\lambda^3 + (K_{pq}^{''}K_{pd}^{''} + \omega_e^2 + K_{iq}^{''} + K_{id}^{''})\lambda^2 \tag{94}$$
$$+ (K_{pq}^{''}K_{id}^{''} + K_{pd}^{''}K_{iq}^{''})\lambda + K_{iq}^{''}K_{id}^{''} = 0$$

If this expression is set equal to a desired characteristic equation

$$\lambda^4 + d_3\lambda^3 + d_2\lambda^2 + d_1\lambda + d_0 = 0 \tag{95}$$

coefficient matching yields the following nonlinear coupled set of equations:

$$K_{pq}^{''} + K_{pd}^{''} = d_3 \tag{96}$$

$$K_{pq}^{''}K_{pd}^{''} + \omega_e^2 + K_{iq}^{''} + K_{id}^{''} = d_2 \tag{97}$$

$$K_{pq}^{''}K_{id}^{''} + K_{pd}^{''}K_{iq}^{''} = d_1 \tag{98}$$

$$K_{iq}^{''}K_{id}^{''} = d_0 \tag{99}$$

A Newton-Raphson algorithm was selected to iteratively solve these equations to find the "double-prime" unknowns from which the actual gains can then be derived. The first step is to re-express (96)-(99) in terms of the following four nonlinear functions:

$$f_3 = K_{pq}^{''} + K_{pd}^{''} - d_3 \tag{100}$$

$$f_2 = K_{pq}^{''}K_{pd}^{''} + \omega_e^2 + K_{iq}^{''} + K_{id}^{''} - d_2 \tag{101}$$

$$f_1 = K_{pq}^{''}K_{id}^{''} + K_{pd}^{''}K_{iq}^{''} - d_1 \tag{102}$$

$$f_0 = K_{iq}^{''}K_{id}^{''} - d_0 \tag{103}$$

The update equation is given by

$$\begin{bmatrix} K_{pq,new}^{''} \\ K_{pd,new}^{''} \\ K_{iq,new}^{''} \\ K_{id,new}^{''} \end{bmatrix} = \begin{bmatrix} K_{pq,old}^{''} \\ K_{pd,old}^{''} \\ K_{iq,old}^{''} \\ K_{id,old}^{''} \end{bmatrix} - \left[\frac{\delta\vec{F}}{\delta\vec{K}^{''}}(K_{old}^{''}) \right]^{-1} \begin{bmatrix} f_3(\vec{K}_{old}^{''}) \\ f_2(\vec{K}_{old}^{''}) \\ f_1(\vec{K}_{old}^{''}) \\ f_0(\vec{K}_{old}^{''}) \end{bmatrix} \tag{104}$$

where $\vec{F} = [f_3, f_2, f_1, f_0]^T$ and $\vec{K}^{''} = [K_{pq}^{''}, K_{pd}^{''}, K_{iq}^{''}, K_{id}^{''}]^T$. The notation $\vec{K}_{old}^{''}$ implies that $\vec{K}^{''}$ is evaluated at the old (or previous) value. The specified Jacobian matrix is given by

$$\frac{\delta \vec{F}}{\delta \vec{K}''}(K''_{old}) = \begin{bmatrix} 1 & 1 & 0 & 0 \\ K''_{pd,old} & K''_{pq,old} & 1 & 1 \\ K''_{id,old} & K''_{iq,old} & K''_{pd,old} & K''_{pq,old} \\ 0 & 0 & K''_{id,old} & K''_{iq,old} \end{bmatrix} \quad (105)$$

C. Design Example

Given the following desired Bessel closed-loop pole locations:

$$\lambda_{1,2} = 8000(-0.6573 \pm j0.8302) = -5258.4 \pm j6641.6 \quad (106)$$

$$\lambda_{3,4} = 8000(-0.9047 \pm j0.2711) = -7237.6 \pm j2168.8 \quad (107)$$

(which provide a closed-loop bandwidth of about 8000rad/sec or 1273Hz), the desired coefficients of the characteristic equation (95) are

$$d_3 = 2.4992000e{+}04 \quad (108)$$

$$d_2 = 2.8108095e{+}08 \quad (109)$$

$$d_1 = 1.6391316e{+}12 \quad (110)$$

$$d_0 = 4.0966232e{+}15 \quad (111)$$

The authors selected a bandwidth of 1300Hz, so that the control would not interact with an assumed switching frequency of at least 20kHz. If additional signal filtering is used (i.e., for the local current measurements), then the control bandwidth may need to be reduced to prevent unwanted interaction with the filters. This would need to be explored via detailed simulation and possibly "tweaked" during implementation. Update equation (104) is run in MATLAB with $\omega_e = 377$ rad/sec yielding the following double-primed gains:

$$K''_{pq} = 1.0485e{+}04 \quad (112)$$

$$K''_{pd} = 1.4507e{+}04 \quad (113)$$

$$K''_{iq} = 7.1686e{+}07 \quad (114)$$

$$K''_{id} = 5.7147e{+}07 \quad (115)$$

Note, equation (104) is not at all parameter dependent and is only a function of the form of the system equation (89). The actual gains for the single-unit controller are determined from

$$K_{pq} = \frac{(L_x + L_L)K''_{pq} - R_L}{K_{pwm}} \quad (116)$$

$$K_{pd} = \frac{(L_x + L_L)K''_{pd} - R_L}{K_{pwm}} \quad (117)$$

$$K_{iq} = \frac{(L_x + L_L)K''_{iq}}{K_{pwm}} \quad (118)$$

$$K_{id} = \frac{(L_x + L_L) K_{id}''}{K_{pwm}} \tag{119}$$

which ARE clearly parameter dependent! Now since current sensors are in the feedback path, K_{pwm} must account for both the sensor gain and the gain through the STPWM modulator ($\frac{V_{dc}}{2 A_t}$).

D. Extension to Two Inverters in Parallel

The results for two inverters in parallel are investigated next. Assuming the following parameters for the system:

$$L_1 = L_2 = 500\,\mu H \tag{120}$$

$$L_L = 510\,\mu H \tag{121}$$

$$R_L = 4\,\Omega \tag{122}$$

and that the single-unit equivalent connection inductance is then

$$L_x = \frac{L_1}{2} = 250\,\mu H \tag{123}$$

the resulting gains are (where the individual inverter control gains are found by doubling the result since we have two in parallel) so that

$$K_{pq1}' = K_{pq2}' = 7.9373 \tag{124}$$

$$K_{iq1}' = K_{iq2}' = 108{,}963 \tag{125}$$

$$K_{pd1}' = K_{pd2}' = 14.0506 \tag{126}$$

$$K_{id1}' = K_{id2}' = 86{,}863 \tag{127}$$

To derive the ACTUAL gains used in units 1 and 2, the PWM and sensor gains must be accounted for

$$K_{pq1} = K_{pq2} = \frac{7.9373}{K_{pwm} K_{sensor}} \tag{128}$$

$$K_{iq1} = K_{iq2} = \frac{108{,}963}{K_{pwm} K_{sensor}} \tag{129}$$

$$K_{pd1} = K_{pd2} = \frac{14.0506}{K_{pwm} K_{sensor}} \tag{130}$$

$$K_{id1} = K_{id2} = \frac{86{,}863}{K_{pwm} K_{sensor}} \tag{131}$$

With (124)-(127) substituted into (75), the following actual eigenvalues are achieved:

$$\lambda_{1,2} = -7{,}943 \pm j\,12{,}445 \tag{132}$$

$$\lambda_{3,4} = -5,258 \pm j6,642 \tag{133}$$

$$\lambda_{5,6} = -7,238 \pm j2,169 \tag{134}$$

$$\lambda_7 = -9,191 \tag{135}$$

$$\lambda_8 = -18,899 \tag{136}$$

Clearly, there is a strong correspondence between the desired pole locations (106)-(107) and those realized. Detailed simulations would next need to be conducted to confirm the dynamic response.

E. Zero-Sequence Control Analysis

The zero-sequence dynamics for two inverters supplying the R-L load are given by

$$\frac{d}{dt} i_{0,1} = \frac{v_{0,1} - v_{0,2}}{L_1 + L_2} \tag{137}$$

$$i_{0,2} = -i_{0,1} \tag{138}$$

Let's consider that only Proportional (P) control is used in the zero-sequence loop, so that

$$v_{0,1} = K_{pwm} K_{p0} (i_{0,1}^* - i_{0,1}) \tag{139}$$

$$v_{0,2} = K_{pwm} K_{p0} (i_{0,2}^* - i_{0,2}) \tag{140}$$

With $i_{0,1}^* = i_{0,2}^* = 0$ and (138), it follows then that

$$v_{0,1} - v_{0,2} = -2 K_{pwm} K_{p0} i_{0,1} \tag{141}$$

which, substituted into (137), yields

$$\frac{d}{dt} i_{0,1} = \frac{-2 K_{pwm} K_{p0}}{L_1 + L_2} i_{0,1} \tag{142}$$

Equation (142) has an eigenvalue at

$$\lambda = \frac{-2 K_{pwm} K_{p0}}{L_1 + L_2} \tag{143}$$

and thus if we select a desired eigenvalue location λ_{des}, the required proportional gain K_{p0} is

$$K_{p0} = \frac{(L_1 + L_2)}{-2 K_{pwm}} \lambda_{des} \tag{144}$$

To account for the sensor gain for the zero-sequence current measurement, (144) would need to be practically restated as

$$K_{p0} = \frac{(L_1 + L_2)}{-2 K_{pwm} K_{sensor}} \lambda_{des} \tag{145}$$

The λ_{des} should be at least on decade away from the radian switching frequency while sufficiently far in the left-half plane to minimize all lower-frequency circulating currents.

F. Extension to Five Inverters in Parallel

If five identical units are placed in parallel, the expressions for the qd-gains become

$$K_{pq} = 5\frac{(\frac{L_1}{5} + L_L)K_{pq}'' - R_L}{K_{pwm} K_{sensor}} \tag{146}$$

$$K_{pd} = 5\frac{(\frac{L_1}{5} + L_L)K_{pd}'' - R_L}{K_{pwm} K_{sensor}} \tag{147}$$

$$K_{iq} = 5\frac{(\frac{L_1}{5} + L_L)K_{iq}''}{K_{pwm} K_{sensor}} \tag{148}$$

$$K_{id} = 5\frac{(\frac{L_1}{5} + L_L)K_{id}''}{K_{pwm} K_{sensor}} \tag{149}$$

where note, the connection inductance L_x must be set equal to the coupling inductance of a single unit divided by five. The resulting gains must have a scale factor or five out front for reasons documented earlier (in particular since the current allocated to a unit is one-fifth that of an equivalent single unit, for the voltages produced to be the same, the gains must be scaled by a factor of five).

To address the design of the zero-sequence control loops for five inverters, consider the following dynamic equations

$$-v_{0,1} + L_c \frac{d}{dt} i_{0,1} - L_c \frac{d}{dt} i_{0,2} + v_{0,2} = 0 \tag{150}$$

$$-v_{0,1} + L_c \frac{d}{dt} i_{0,1} - L_c \frac{d}{dt} i_{0,3} + v_{0,3} = 0 \tag{151}$$

$$-v_{0,1} + L_c \frac{d}{dt} i_{0,1} - L_c \frac{d}{dt} i_{0,4} + v_{0,4} = 0 \tag{152}$$

$$-v_{0,1} + L_c \frac{d}{dt} i_{0,1} - L_c \frac{d}{dt} i_{0,5} + v_{0,5} = 0 \tag{153}$$

where an identical coupling inductance L_c is assumed for simplicity. It also follows that since the load is wye-connected, one zero-sequence current is algebraically related to the others. If we choose to solve for $i_{0,5}$, we get

$$i_{0,5} = -i_{0,1} - i_{0,2} - i_{0,3} - i_{0,4} \tag{154}$$

If we assume a similar proportional control for each zero-sequence loop, then it follows that

$$v_{0,1} = K_{pwm} K_{p0}(i_{0,1}^* - i_{0,1}) \tag{155}$$

$$v_{0,2} = K_{pwm} K_{p0}(i_{0,2}^* - i_{0,2}) \tag{156}$$

$$v_{0,3} = K_{pwm} K_{p0} (i_{0,3}^* - i_{0,3})$$
(157)

$$v_{0,4} = K_{pwm} K_{p0} (i_{0,4}^* - i_{0,4})$$
(158)

$$v_{0,5} = K_{pwm} K_{p0} (i_{0,5}^* - i_{0,5})$$
(159)

Since it is desired that $i_{0,1}^* = i_{0,2}^* = i_{0,3}^* = i_{0,4}^* = i_{0,5}^* = 0$, substituting (154)-(159) into (150)-(153) and placing the result into state-space normal form yields

$$\frac{d}{dt} \begin{bmatrix} i_{0,1} \\ i_{0,2} \\ i_{0,3} \\ i_{0,4} \end{bmatrix} = \begin{bmatrix} \dfrac{-K_{pwm} K_{p0}}{L_c} & 0 & 0 & 0 \\ 0 & \dfrac{-K_{pwm} K_{p0}}{L_c} & 0 & 0 \\ 0 & 0 & \dfrac{-K_{pwm} K_{p0}}{L_c} & 0 \\ 0 & 0 & 0 & \dfrac{-K_{pwm} K_{p0}}{L_c} \end{bmatrix} \begin{bmatrix} i_{0,1} \\ i_{0,2} \\ i_{0,3} \\ i_{0,4} \end{bmatrix}$$
(160)

The characteristic equation for (160) is simply

$$(\lambda + \frac{K_{pwm} K_{p0}}{L_c})(\lambda + \frac{K_{pwm} K_{p0}}{L_c})(\lambda + \frac{K_{pwm} K_{p0}}{L_c})(\lambda + \frac{K_{pwm} K_{p0}}{L_c}) = 0$$
(161)

and so all four roots are co-located at

$$\lambda_{1,2,3,4} = \frac{-K_{pwm} K_{p0}}{L_c}$$
(162)

which is identical to (143) with $L_1 = L_2$. Therefore, the zero-sequence gain formula (144) would continue to hold for five inverters in parallel. Repeating that equation (assuming equal combining/coupling inductances)

$$K_{p0} = \frac{-L_c \lambda_{des}}{K_{pwm} K_{sensor}}$$
(163)

where the impact of the feedback current sensor gain has been incorporated.

IV. INDUCTION MACHINE LOAD ANALYSIS

One of the goals of this research is to facilitate the development of motor controllers employing multiple paralleled power inverters. The following analysis will extend the R-L load results to an induction motor drive and, in a later section, to a permanent-magnet synchronous machine drive. The stator voltage equations of the three-phase symmetrical induction machine represented in the synchronous reference frame are given by

$$v_{qs}^e = r_s i_{qs}^e + \frac{\omega_e}{\omega_b} \psi_{ds}^e + \frac{1}{\omega_b} \frac{d}{dt} \psi_{qs}^e \tag{164}$$

$$v_{ds}^e = r_s i_{ds}^e - \frac{\omega_e}{\omega_b} \psi_{qs}^e + \frac{1}{\omega_b} \frac{d}{dt} \psi_{ds}^e \tag{165}$$

where r_s is the per-phase stator resistance, ω_b is the base (rated) electrical angular frequency, and ψ represents flux linkages per second. The stator flux linkages per second may be expressed in terms of the stator leakage flux and the air-gap flux by

$$\psi_{qs}^e = X_{ls} i_{qs}^e + \psi_{mq}^e \tag{166}$$

$$\psi_{ds}^e = X_{ls} i_{ds}^e + \psi_{md}^e \tag{167}$$

where the air-gap flux linkages per second are given by

$$\psi_{mq}^e = X_m (i_{qs}^e + i_{qr}'^e) \tag{168}$$

$$\psi_{md}^e = X_m (i_{ds}^e + i_{dr}'^e) \tag{169}$$

The parameters X_{ls} and X_m are the stator leakage and magnetizing reactances, respectively (each a constant evaluated at ω_b). The prime in (168)-(169) denotes that a rotor variable is a referred quantity (that is, the rotor windings have been mathematically replaced by equivalent windings with the same number of turns as the stator windings). The referred rotor flux linkages per second are given by

$$\psi_{qr}'^e = X_{lr}' i_{qr}'^e + \psi_{mq}^e \tag{170}$$

$$\psi_{dr}'^e = X_{lr}' i_{dr}'^e + \psi_{md}^e \tag{171}$$

where X_{lr}' is the referred rotor leakage reactance (a constant). Solving (170)-(171) for $i_{qr}'^e$ and $i_{dr}'^e$, substituting the results into (168)-(169) and collecting the ψ_{mq}^e and ψ_{md}^e terms yields

$$\psi_{mq}^e = \frac{X_m X_{lr}'}{X_m + X_{lr}'} \left[i_{qs}^e + \frac{\psi_{qr}'^e}{X_{lr}'} \right] \tag{172}$$

$$\psi_{md}^e = \frac{X_m X_{lr}'}{X_m + X_{lr}'} \left[i_{ds}^e + \frac{\psi_{dr}'^e}{X_{lr}'} \right] \tag{173}$$

Finally, substituting (172)-(173) into (166)-(167) gives

$$\psi_{qs}^e = X'' i_{qs}^e + \psi_q'' \tag{174}$$

$$\psi_{ds}^e = X'' i_{ds}^e + \psi_d'' \tag{175}$$

where the double-prime quantities are given by

$$X'' = X_{ls} + \frac{X_m X_{lr}'}{X_m + X_{lr}'} \tag{176}$$

$$\psi_q'' = \frac{X_m}{X_m + X_{lr}'} \psi_{qr}'^e \tag{177}$$

$$\psi_d'' = \frac{X_m}{X_m + X_{lr}'} \psi_{dr}'^e \tag{178}$$

The stator voltage equations (164)-(165) may then be re-expressed as

$$v_{qs}^e = r_s i_{qs}^e + \frac{\omega_e}{\omega_b}(X'' i_{ds}^e + \psi_d'') + \frac{1}{\omega_b}\frac{d}{dt}(X'' i_{qs}^e + \psi_q'') \tag{179}$$

$$v_{ds}^e = r_s i_{ds}^e - \frac{\omega_e}{\omega_b}(X'' i_{qs}^e + \psi_q'') + \frac{1}{\omega_b}\frac{d}{dt}(X'' i_{ds}^e + \psi_d'') \tag{180}$$

The current control dynamics are desired to be very fast. As a result, the slowly-varying rotor variables may be assumed to be constant while considering the stator dynamics. This implies that

$$\frac{d}{dt}\psi_{qr}'^e = \frac{d}{dt}\psi_{dr}'^e = 0 \tag{181}$$

which observing (177)-(178) requires that

$$\frac{d}{dt}\psi_q'' = \frac{d}{dt}\psi_d'' = 0 \tag{182}$$

Furthermore, assuming the drive is vector controlled ensures that

$$\psi_{qr}'^e = 0 \tag{183}$$

$$\psi_{dr}'^e = \psi_{dr}'^{e*} \tag{184}$$

Substituting (182)-(184) into (179)-(180) yields

$$v_{qs}^e = r_s i_{qs}^e + \frac{\omega_e}{\omega_b} X'' i_{ds}^e + \frac{\omega_e}{\omega_b}\frac{X_m}{X_m + X_{lr}'}\psi_{dr}'^{e*} + \frac{X''}{\omega_b}\frac{d}{dt}i_{qs}^e \tag{185}$$

$$v_{ds}^e = r_s i_{ds}^e - \frac{\omega_e}{\omega_b} X'' i_{qs}^e + \frac{X''}{\omega_b}\frac{d}{dt}i_{ds}^e \tag{186}$$

If we let

$$L'' = \frac{X''}{\omega_b} \tag{187}$$

and merge these equations with the qd-equations for a single inverter with coupling inductor (81)-(82), we find

$$-v_q^e + L_x \frac{d}{dt} i_{qs}^e + L_x \omega_e i_{ds}^e + r_s i_{qs}^e + \omega_e L'' i_{ds}^e \qquad (188)$$

$$+ \frac{\omega_e}{\omega_b} \frac{X_m}{X_m + X_{lr}'} \psi_{dr}^{'e*} + L'' \frac{d}{dt} i_{qs}^e = 0$$

$$-v_d^e + L_x \frac{d}{dt} i_{ds}^e - L_x \omega_e i_{qs}^e + r_s i_{ds}^e - \omega_e L'' i_{qs}^e \qquad (189)$$

$$+ L'' \frac{d}{dt} i_{ds}^e = 0$$

If we next observe that the PI-control equations are

$$v_q^e = K_{pq}'(i_{qs}^{e*} - i_{qs}^e) + K_{iq}' x_q^e \qquad (190)$$

$$v_d^e = K_{pd}'(i_{ds}^{e*} - i_{ds}^e) + K_{id}' x_d^e \qquad (191)$$

$$\frac{d}{dt} x_q^e = i_{qs}^{e*} - i_{qs}^e \qquad (192)$$

$$\frac{d}{dt} x_d^e = i_{ds}^{e*} - i_{ds}^e \qquad (193)$$

placing (188)-(193) in state-space normal form gives

$$\frac{d}{dt} \begin{bmatrix} i_{qs}^e \\ i_{ds}^e \\ x_q^e \\ x_d^e \end{bmatrix} = \begin{bmatrix} -K_{pq}'' & -\omega_e & K_{iq}'' & 0 \\ \omega_e & -K_{pd}'' & 0 & K_{id}'' \\ -1 & 0 & 0 & 0 \\ 0 & -1 & 0 & 0 \end{bmatrix} \begin{bmatrix} i_{qs}^e \\ i_{ds}^e \\ x_q^e \\ x_d^e \end{bmatrix} \qquad (194)$$

$$+ \begin{bmatrix} K_{pq}'' & 0 \\ 0 & K_{pd}'' \\ 1 & 0 \\ 0 & 1 \end{bmatrix} \begin{bmatrix} i_{qs}^{e*} \\ i_{ds}^{e*} \end{bmatrix} + \frac{-\omega_e X_m \psi_{dr}^{'e*}}{\omega_b (L_x + L'')(X_m + X_{lr}')} \begin{bmatrix} 1 \\ 0 \\ 0 \\ 0 \end{bmatrix}$$

where in this case

$$K_{pq}'' = \frac{r_s + K_{pq}'}{L_x + L''} \qquad (195)$$

$$K_{pd}'' = \frac{r_s + K_{pd}'}{L_x + L''} \qquad (196)$$

$$K_{iq}'' = \frac{K_{iq}'}{L_x + L''} \qquad (197)$$

$$K_{id}'' = \frac{K_{id}'}{L_x + L''} \qquad (198)$$

Note, this is the same form as equations (89)-(94) where the stator resistance (r_s) has replaced the load resistance and the stator substransient inductance (L'') has replaced the load inductance. Thus, the solution may progress as before: use the Newton-Raphson to

solve for the double-primed gains, use (195)-(198) to derive the primed gains, and finally divide those quantities by $K_{pwm} K_{sensor}$ to establish the gains for the single aggregate inverter. Those gains are then scaled by the required number of inverters to calculate the individual inverter current control parameters.

IV. PERMANENT-MAGNET SYNCHRONOUS MACHINE LOAD ANALYSIS

The derivation of the control equations for a round-rotor permanent-magnet synchronous motor (PMSM) is more straight-forward. The PMSM is modeled in the rotor reference frame by

$$v_{qs}^r = r_s i_{qs}^r + L_{ss} \frac{d}{dt} i_{qs}^r + \omega_r L_{ss} i_{ds}^r + \omega_r \lambda_m^{'r} \tag{199}$$

$$v_{ds}^r = r_s i_{ds}^r + L_{ss} \frac{d}{dt} i_{ds}^r - \omega_r L_{ss} i_{qs}^r \tag{200}$$

These equations assume negligible cogging torque and sinusoidal back emf. The parameter r_s is the per-phase stator resistance, L_{ss} is the stator self inductance (leakage plus magnetizing), and $\lambda_m^{'r}$ is the peak flux linkage between the permanent magnet and the stator windings. The inverter equations in the rotor reference frame are similar to what we had previously except now the angle in (13) is the rotor electrical angle, superscript 'e' is replaced by superscript 'r', and ω_e is replaced by the rotor electrical angular velocity ω_r. Coupling the inverter dynamics in the rotor reference frame (81)-(82) to the machine equations yields:

$$-v_q^r + L_x \frac{d}{dt} i_{qs}^r + L_x \omega_r i_{ds}^r + r_s i_{qs}^r \tag{201}$$

$$+ L_{ss} \frac{d}{dt} i_{qs}^r + \omega_r L_{ss} i_{ds}^r + \omega_r \lambda_m^{'r} = 0$$

$$-v_d^r + L_x \frac{d}{dt} i_{ds}^r - L_x \omega_r i_{qs}^r + r_s i_{ds}^r \tag{202}$$

$$+ L_{ss} \frac{d}{dt} i_{ds}^r - \omega_r L_{ss} i_{qs}^r = 0$$

These equations may then be combined with the PI-current control equations in the rotor reference frame

$$v_q^r = K_{pq}'(i_{qs}^{r*} - i_{qs}^r) + K_{iq}' x_q^r \tag{203}$$

$$v_d^r = K_{pd}'(i_{ds}^{r*} - i_{ds}^r) + K_{id}' x_d^r \tag{204}$$

$$\frac{d}{dt} x_q^r = i_{qs}^{r*} - i_{qs}^r \tag{205}$$

$$\frac{d}{dt} x_d^r = i_{ds}^{r*} - i_{ds}^r \tag{206}$$

to yield the state-space description

$$\frac{d}{dt}\begin{bmatrix} i_{qs}^r \\ i_{ds}^r \\ x_q^r \\ x_d^r \end{bmatrix} = \begin{bmatrix} -K_{pq}^{''} & -\omega_r & K_{iq}^{''} & 0 \\ \omega_r & -K_{pd}^{''} & 0 & K_{id}^{''} \\ -1 & 0 & 0 & 0 \\ 0 & -1 & 0 & 0 \end{bmatrix} \begin{bmatrix} i_{qs}^r \\ i_{ds}^r \\ x_q^r \\ x_d^r \end{bmatrix} \qquad (207)$$

$$+ \begin{bmatrix} K_{pq}^{''} & 0 \\ 0 & K_{pd}^{''} \\ 1 & 0 \\ 0 & 1 \end{bmatrix} \begin{bmatrix} i_{qs}^{r*} \\ i_{ds}^{r*} \end{bmatrix} + \begin{bmatrix} \dfrac{-\omega_r \lambda_m^{'r}}{L_x + L_{ss}} \\ 0 \\ 0 \\ 0 \end{bmatrix}$$

where in this case

$$K_{pq}^{''} = \frac{r_s + K_{pq}^{'}}{L_x + L_{ss}} \qquad (208)$$

$$K_{pd}^{''} = \frac{r_s + K_{pd}^{'}}{L_x + L_{ss}} \qquad (209)$$

$$K_{iq}^{''} = \frac{K_{iq}^{'}}{L_x + L_{ss}} \qquad (210)$$

$$K_{id}^{''} = \frac{K_{id}^{'}}{L_x + L_{ss}} \qquad (211)$$

Note, once again this is the same form as equations (89)-(94) where R_L is replaced by r_s and L_L is replaced by L_{ss}. Thus, the solution may progress as in the R-L case: use the Newton-Raphson routine to solve for the double-prime gains, use (208)-(211) and the equivalent connection inductance to solve for the primed gains, and divide those quantities by $K_{pwm} K_{sensor}$ to arrive at the actual gains for a single aggregate inverter. Those gains are then scaled by the required number of paralleled inverters.

VI. VECTOR CONTROL IMPLEMENTATION

Vector control is the state-of-the-art means of controlling AC machines. It essentially gives the AC machine the torque characteristics of a DC commutator machine -- notably, near-instantaneous torque response (as quick as the machine currents can be changed and tracked). The following equations are included to document how the inverter control development presented thus far can be extended to a high-performance servo application. We will start first with the induction machine.

A. Induction Machine Vector Control

The induction machine vector control may be implemented directly (by physically locating the position of the rotor flux and placing the synchronous reference frame d-axis there) or indirectly (by using the induction machine governing equations to establish a necessary and sufficient condition to guarantee that all of the rotor flux is directed along the synchronous reference frame d-axis).

1. Direct method of vector control

The direct method of vector control can either use air-gap flux measurement or simply stator voltage and current measurements. If sense coils are used to establish the air-gap flux (by integrating the resultant coil voltages), then we can establish the required synchronous reference frame angle by the following sequence of calculations:

$$i_{qs}^s = i_{as} \tag{212}$$

$$i_{ds}^s = -\frac{1}{\sqrt{3}} i_{as} - \frac{2}{\sqrt{3}} i_{bs} \tag{213}$$

$$\psi_{qr}^{'s} = \frac{X_{rr}'}{X_m} \psi_{mq}^s - X_{lr}' i_{qs}^s \tag{214}$$

$$\psi_{dr}^{'s} = \frac{X_{rr}'}{X_m} \psi_{md}^s - X_{lr}' i_{ds}^s \tag{215}$$

$$\psi_{r,pk}' = \sqrt{(\psi_{qr}^{'s})^2 + (\psi_{dr}^{'s})^2} \tag{216}$$

$$\theta_e^* = \tan^{-1}\left[\frac{\psi_{qr}^{'s}}{\psi_{dr}^{'s}}\right] \tag{217}$$

Notably, the approach has issues at low-frequency due to the requirement of integrating to find the air-gap flux linkage components.

An alternative scheme does not require special air-gap sensors, but only simple current and voltage measurements. It establishes the required synchronous reference frame angle by first calculating the stationary reference frame voltages and currents from the physical variables:

$$i_{qs}^s = i_{as} \tag{218}$$

$$i_{ds}^s = -\frac{1}{\sqrt{3}} i_{as} - \frac{2}{\sqrt{3}} i_{bs} \tag{219}$$

$$v_{qs}^s = v_{as} \tag{220}$$

$$v_{ds}^s = -\frac{1}{\sqrt{3}} v_{as} - \frac{2}{\sqrt{3}} v_{bs} \tag{221}$$

The stator flux linkages per second (in the stationary reference frame) are then found by integrating the governing equations:

$$\psi_{qs}^s = \int_0^t (-r_s \omega_b i_{qs}^s + \omega_b v_{qs}^s) d\zeta \tag{222}$$

$$\psi_{ds}^s = \int_0^t (-r_s \omega_b i_{ds}^s + \omega_b v_{ds}^s) d\zeta \tag{223}$$

This again imposes a DSP difficulty at low frequencies. The referred rotor flux linkages are then determined by

$$\psi_{qr}^{'s} = \frac{X_{rr}'}{X_m} \left[\psi_{qs}^s - (X_{ss} - \frac{X_m^2}{X_{rr}'}) i_{qs}^s \right] \tag{224}$$

$$\psi_{dr}^{'s} = \frac{X_{rr}'}{X_m} \left[\psi_{ds}^s - (X_{ss} - \frac{X_m^2}{X_{rr}'}) i_{ds}^s \right] \tag{225}$$

$$\psi_{r,pk}' = \sqrt{(\psi_{qr}^{'s})^2 + (\psi_{dr}^{'s})^2} \tag{226}$$

The d-axis is placed on top of the rotor d-flux in the synchronous reference frame by assigning

$$\theta_e^* = \tan^{-1} \left[\frac{\psi_{qr}^{'s}}{\psi_{dr}^{'s}} \right] \tag{227}$$

2. Indirect method of vector control

Alternatively, the desired synchronous reference frame angle may be derived by only measuring the rotor electrical angular position, where this relates to the mechanical angle by

$$\theta_r = \frac{P}{2} \theta_{rm} \tag{228}$$

where P is the number of poles. Then θ_e^* is established from a necessary and sufficient condition

$$\theta_e^* = \theta_r + \int_0^t \left[\frac{\omega_b r_r' X_m i_{qs}^{e*}}{X_{rr}' \psi_{dr}^{'e*}} \right] d\zeta \tag{229}$$

where $\psi_{dr}^{'e*}$ is the desired d-axis rotor flux and i_{qs}^{e*} is the desired q-axis stator current, both in

the synchronous reference frame. If the desired rotor flux magnitude is kept constant, then it follows that

$$\psi_{dr}^{'e*} = X_m i_{ds}^{e*} \tag{230}$$

and (229) simplifies to

$$\theta_e^* = \theta_r + \int_0^t \left[\frac{\omega_b r_r' i_{qs}^{e*}}{X_{rr}' i_{ds}^{e*}} \right] d\zeta \tag{231}$$

Thus it requires only position feedback information and feedforward of the commanded stator currents in the synchronous reference frame.

B. Permanent-Magnet Synchronous Machine

Field-oriented vector control for a PMSM is achieved through self-synchronization (feeding back θ_r and setting it equal to θ_e^*) and setting i_{ds}^{r*} equal to zero. The commanded q-axis stator current will then be directly proportional to the developed electromagnetic torque.

VII. OUTER SPEED LOOP DESIGN

A perspective outer speed control loop for a vector-controlled induction machine or PMSM may take the form illustrated in Figure 7. That is under vector control, the developed electromagnetic torque is related to the commanded q-stator current for an induction machine by

$$T_e = \frac{3 P X_m \psi_{dr}^{'e*}}{4 \omega_b X_{rr}'} i_{qs}^{e*}$$

(232)

and for a round-rotor PMSM by

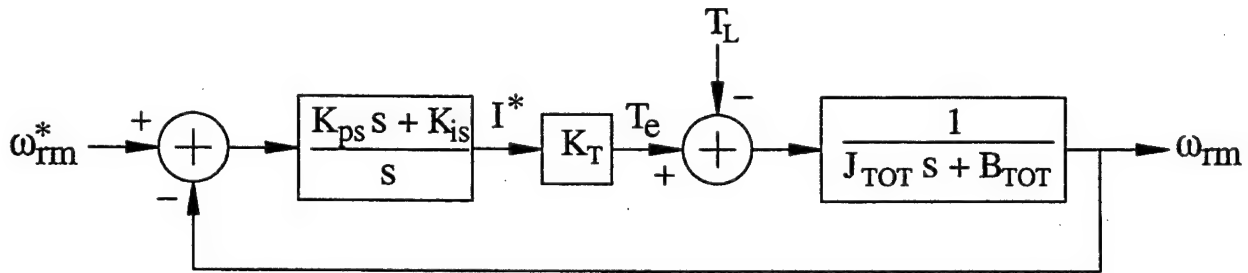$$T_e = \frac{3 P \lambda_m^{'r}}{4} i_{qs}^{r*}$$

(233)

Figure 7. Closed-loop speed control system

By inspection of (232)-(233), the appropriate value for K_T in Figure 7 may be found. The closed-loop transfer function for the control loop of Figure 7 is given by

$$G_{CL}(s) = \frac{K_t K_{ps} s + K_t K_{is}}{J_{TOT} s^2 + (B_{TOT} + K_t K_{ps}) s + K_t K_{is}}$$

(234)

where J_{TOT} represents the combined inertia of motor and load, B_{TOT} is the combined viscous friction or motor and load, and K_{ps} and K_{is} are the PI-control gains. By specifying the dynamics of the speed loop (through a pair of desired pole locations), the two gains may be uniquely determined. The pole locations are best selected at least one decade away from the current control pole locations to avoid unwanted interaction. The zero in (234) may impact the response unfavorably by introducing more overshoot than desired. One potential solution is to insert a pre-filter after the commanded speed signal. For a pre-filter choice of

$$G_{pf}(s) \ = \ \dfrac{1}{\dfrac{K_{ps}}{K_{is}} s \ + \ 1} \tag{235}$$

the zero is canceled. Obviously, detailed simulation should be used in conjunction with these design suggestions to investigate interaction and non-idealities in full.

$$G_{pf}(s) \ = \ \dfrac{1}{\dfrac{K_{ps}}{K_{is}} s \ + \ 1} \tag{235}$$

VIII. CONCLUSION

The research effort documented in this technical report provides analysis/synthesis tools for choosing feedback gains for a set of paralleled inverters. The local control is set forth in a synchronous reference frame and also addresses the question of circulating zero-sequence currents. The procedure for a generic R-L load was extended to both an induction motor load and a permanent-magnet synchronous machine load. Interestingly, a similar set of equations was found to be applicable in each case. The resulting inner current control design was then mapped outward, in the case of the machine loads, to facilitate the design of a speed-control drive. To make the analysis comprehensive, equations for the vector control implementation options were presented and the resultant simple PI-control loop analyzed.

In order to validate the control procedures outlined here, the dynamic equations for the R-L load, induction motor, and PMSM, together with the inverters, must be simulated in detail using a program such as ACSL. Such simulations could be structured to model slight differences between the units and thus study the efficacy of the circulating current control. Also, the interaction between sensor/filter dynamics and the current control dynamics may be more accurately studied and a more informed decision made about the suitability of the current control bandwidth. Finally, simulation would allow the study of the vector control implementations and any sort of speed control loop. The preceding research effort must next be applied to a hardware testbed, where the individual programming the DSP control must work closely with the modeler/simulator to accurately test each stage of development.

Ultimately, the above approach could be extended to a propulsion-type application of a high-bandwidth low-power inverter module (consisting of paralleled units) operating in parallel with a low-bandwidth (slower switching) high-power inverter module. The efficacy of using the high-bandwidth unit to improve the fidelity of the output waveforms could then be evaluated.

IX. REFERENCES

[1] Chandorkar, M., Divan, D., Adapa, R., "Control of Parallel Connected Inverters in Stand-Alone AC Supply Systems," IEEE Transactions on Industry Applications, vol 29, pp 136-143, Feb 1993.

[2] Kawabata, T., Higashino, S., "Parallel Operation of Voltage Source Inverters," IEEE Transactions on Industry Applications, vol 24, No 2, Mar/Apr 1988.

[3] Chen, J., Chu, C., "Combination Voltage-Controlled and Current-Controlled PWM Inverters for Parallel Operation of UPS," IEEE Trans. on Power Electronics, Vol 10, pp 547-558, 1995.

[4] Holtz, J., Lotzkat, W, Werner, K., "A High-Power Multi Transistor-Inverter Uninterruptible Power Supply System," IEEE Trans. Power Electron., Vol 3, pp 278-285, 1988.

[5] Holtz, J., Werner K., "Multi-Inverter UPS System with Redundant Load Sharing Control," IEEE Trans. Indust. Electron., Vol 37, No. 6, pp. 506-513, Dec 1990.

[6] Chen, J., Chu, C., Huang, C., "The Parallel Operation of two UPS by the Coupled-Inductor Method," IEEE IE Conf. Rec., 1992, pp 733-736.

[7] Siri, K., Lee, C., "Current Distribution Control of Converter Connected in Parallel," IEEE IAS Conf. Rec., 1990, pp 1274-1280.

[8] Okuma, S., Iwata, K., Suzuki, K., "Parallel Running of GTO PWM Inverters," IEEE 1984, pp 111-120.

[9] Tamai, S., Kinoshita, M., "Parallel Operation of Digital Controlled UPS System," IECON '91, Vol 2, Nov 1993, pp 326-331.

[10] Hur, N, Nam, K., "A Robust Load-Sharing Control Scheme for Parallel Connected Multisystems," IEEE Trans. Indust. Electron., Vol 47, No. 4, Aug 2000, pp 871-879.

[11] Wu, T., Chen, Y., Huang, Y., "3C Strategy for Inverters in Parallel Operation Achieving an Equal Current Distribution," IEEE Trans. Indust. Electron., Vol 47, No. 2, Apr 2000, pp 273-281.

[12] Siri, K., Wu, T., Lee, C., "Current Distribution Control Schemes for Parallel Connected Converter Modules Part I: Master-Slave Control," IEEE Trans. Aerospace Electron. Sys., Vol 28, pp 829-840, July 1995.

[13] Siri, K., Wu, T., Lee, C., "Current Distribution Control Schemes for Parallel Connected Converter Modules Part II: Central-Limit Control," IEEE Trans. Aerospace Electron. Sys., Vol 28, pp 841-851, July 1995.

[14] Tuladhar, A., Jin, H., Unger, T., Mauch, K., "Control of Parallel Inverters in

Distributed AC Power Systems with Consideration of Line Impedance Effects," IEEE Trans. on Industry Applications, Vol 36, No. 1, Jan/Feb 2000, pp 131-138.

[15] Meng, Y., Duan, S., Kang, Y., Chen, J., "Research on Voltage Source Inverters with Wireless Parallel Operation," Proceedings of the Power Elec. and Motion Control Conference 2000, Vol 2, pp 808-812.

[16] Coelho, E., Cortizo, P., Garcia, P., "Small Signal Stability for Parallel Connected Inverters in Stand-Alone AC Supply Systems," Industry Applications Conf. Rec, 2000, Vol 4, pp 2345-2352.

[17] Fukuda, S., Matsushita, K., "A Control Method for Parallel-Connected Multiple Inverter Systems," Power Elect. and Variable Speed Drives Conf. Rec., 1998, pp 175-180.

[18] Prodanovic, M., Green, T., Mansir, H., "A Survey of Control Methods for Three-Phase Inverters in Parallel Connection," Power Elect. and Variable Speed Drives Conf. Rec., 2000, pp 472-477.

[19] Matsui, K., Kawata, Y., Veda, F., "Application of Parallel Connected NPC-PWM Inverters with Multi-Level Modulation for AC Motor Drive," IEEE Trans. on Power Electronics, Vol 5, Sep 2000, pp 901-907.

[20] Shanxu, D., Yu, M., Jian, X., Yong, K., Jian, C., "Parallel Operation Control Techniques of Voltage Source Inverters in UPS," Proceedings of Power Electronics and Drive Systems 1999, pp 883-887.

[21] Xiong, R., Hao, W., Chen, T., "A Study of Parallel Operation Control Techniques of DC/AC SPWM Inverter," Proceedings of Power Electronics and Drive Systems 1999, pp 1027-1032.

[22] Krause, P., Wasynczuk, O., Sudhoff, S., Analysis of Electric Machinery, McGraw-Hill, New York, 1986.

[23] Novotny, D., Lipo, T., Vector Control and Dynamics of AC Drives, Oxford University Press, New York, 1997.

[24] Mohan, N., Undeland, T., Robbins, W., Power Electronics, John Wiley & Sons, New York, 1995.

[25] Ciezki, J., Ashton, R., "PEBB Feedback Control Law Library Volume 1: Three-Phase Inverter Control Algorithms," Naval Postgraduate School Technical Report, Prepared for: Naval Surface Warfare Center Annapolis Det., January 1999.

[26] Thunes, J., Kerkman, R., Schlegel, D., Rowan, T., "Current Regulator Instabilities on Parallel Voltage-Source Inverters," IEEE Trans. on Indust. App., Vol 35, No 1, Jan/Feb 1999, pp 70-77.

[27] Ye, Z., Boroyevich, D., Lee, F., "Modeling and Control of Zero-Sequence Currents in Parallel Multi-Phase Converters," Power Elect. Spec. Conf., Vol 2, pp 680-685.

[28] Yoshikawa, T., Inaba, H., Mine, T., "Analysis of Parallel Operation Methods of PWM Inverter Sets for an Ultra-High Speed Elevator," Applied Power Elec. Conf., Vol 2, pp 944-950.

[29] Sukegawa, T., et al, "A Multiple PWM GTO Line-Side Converter for Unity Power Factor and Reduced Harmonics," IEEE Trans. on Indust. App., Vol 28, No 6, Nov/Dec 1992, pp 1302-1308.

[30] Ogasawara, S., Takagaki, J., Akagi, H., "A Novel Control Scheme of a Parallel Current-Controlled PWM Inverter," IEEE Trans. on Indust. App., Vol 28, No 5, Sep/Oct 1992, pp 1023-1030.

[31] Matakas, L., Masada, E., "Multi-Converter Implementation by Parallel Association of K Voltage Source Converters - Control Method," EPE '93, pp 35-40.

[32] Zhao, Y., Lipo, T., "Space Vector PWM Control of Dual Three-Phase Induction Machine Using Vector Space Decomposition," IEEE Trans. on Indust. App., Vol 31, No 5, Sep/Oct 1995, pp 1100-1109.

[33] Komatsuzaki, "Cross Current Control for Parallel Operating Three-Phase Inverter," PESC '94, pp 943-950.

[34] Halasz, G., Csonka, G., Hassan, A., "Sinusoidal PWM Techniques with Additional Zero-Sequence Harmonics," IECON '94, pp 85-90.

[35] Xing, K., Lee, F., Boroyevich, D., Ye, Z., Mazumder, S., "Interleaved PWM with Discontinuous Space Vector Modulation," IEEE Trans. on Power Elec., Vol 14, No. 5, Sep 1999, pp 982-989.

[36] Matakas, L., Kaiser, W., "Low Harmonics, Decoupled Histeresis Type Current Control of a Multi-Converter Consisting of a Parallel Transformerless Connection of VSC Converters," IAS '97, pp 1633-1640.

INITIAL DISTRIBUTION LIST

No. Copies

1. Defense Technical Information Center   2
   8725 John J. Kingman Rd, STE 0944
   Ft. Belvoir, VA 22060-6218

2. Dudley Knox Library, Code 52   2
   Naval Postgraduate School
   411 Dyer Road
   Monterey, CA 93943-5101

3. Research Office, Code 09   1
   Naval Postgraduate School
   589 Dyer Road
   Monterey, CA 93943-5138

4. Chairman, Code EC   1
   Department of Electrical and Computer Engineering
   Naval Postgraduate School
   833 Dyer Road
   Monterey, CA 93943-5121

5. Professor John Ciezki, Code EC/Cy   3
   Department of Electrical and Computer Engineering
   Naval Postgraduate School
   833 Dyer Road
   Monterey, CA 93943-5121

6. Professor Robert Ashton, Code EC/Ah   3
   Department of Electrical and Computer Engineering
   Naval Postgraduate School
   833 Dyer Road
   Monterey, CA 93943-5121

7. Naval Surface Warfare Center Carderock Division   1
   Attn: Tom Fikse
   Code 812, Building 77L
   Philadelphia Naval Business Center
   Philadelphia, PA 19112-5083

8. Naval Surface Warfare Center Carderock Division   2
   Attn: Lynn Petersen
   Code 812, Building 77L
   Philadelphia Naval Business Center
   Philadelphia, PA 19112-5083

9. Naval Surface Warfare Center Carderock Division   1
   Attn: Joe Borraccini
   Code 813, Building 77L
   Philadelphia Naval Business Center
   Philadelphia, PA 19112-5083

10. Naval Surface Warfare Center Carderock Division   1
    Attn: Michael Golda
    Code 81, Building 77L
    Philadelphia Naval Business Center
    Philadelphia, PA 19112-5083